Supporting Information

Bimetallic Pt_xCo_y nanoparticles with curved faces for highly efficient hydrogenation of cinnamaldehyde

Yan Gu,[a,b] Yonghui Zhao,*[a] Panpan Wu,[b] Bo Yang,*[b] Nating Yang,[a] and Yan Zhu*[a,b]

[a] CAS Key Laboratory of Low-Carbon Conversion Science and Engineering, Shanghai Advanced Research Institute, Chinese Academy of Sciences, Shanghai 201210, PR China

[b] School of Physical Science and Technology, ShanghaiTech University, Shanghai 201210, PR China

Experimental details:

Synthesis of PtCo nanoparticles with curved faces exposed (710) facets: Under argon flow, [$Pt(acac)_2$] (0.05 mmol), [$Co(acac)_2$] (0.012 mmol), oleylamine (9 mL), benzoic acid (0.316 mmol) and diphenyl ether (1mL) were mixed in a 25 mL three-necked, round-bottom flask with a magnetic stirrer. The flask was immersed in an oil bath at 130 ^oC, and the reaction mixture turned into a transparent solution at this temperature for 3 min. The flask was then transferred to a second oil bath at 210 ^oC under carbon monoxide gas. The typical flow rate of CO gas was set at 220 mL/min and the reaction time was 30 min. The products were separated by centrifugation at 6000 rpm for 5 min and further purified by washing with ethanol three times.

Synthesis of PtCo nanoparticles with curved faces exposed (420) facets: Under argon flow, [$Pt(acac)_2$] (0.05 mmol), [$Co(acac)_2$] (0.028 mmol), oleylamine (9 mL), and benzoic acid (0.316 mmol) or 1-adamantaneacetic acid (0.319 mmol) or cyclohexanecarboxylic acid (0.316 mmol) were mixed in a 25 mL three-necked, round-bottom flask with a magnetic stirrer. The flask was immersed in an oil bath at 130 ^oC, and the reaction mixture turned into a transparent solution at this temperature

for 3 min. The flask was then transferred to a second oil bath at 210 °C under carbon monoxide gas. The typical flow rate of CO gas was set at 220 mL/min and the reaction time was 30 min. The products were separated by centrifugation at 6000 rpm for 5 min and further purified by washing with ethanol three times.

Synthesis of PtCo nanoparticles with curved faces exposed (110) facets: Under argon flow, [$Pt(acac)_2$] (0.05 mmol), [$Co(acac)_2$] (0.014 mmol), oleylamine (9 mL), and octadecanoic acid (0.316 mmol) or lauric acid (0.316 mmol) were mixed in a 25 mL three-necked, round-bottom flask with a magnetic stirrer. The flask was immersed in an oil bath at 130 °C, and the reaction mixture turned into a transparent solution at this temperature at this temperature for 3 min. The flask was then transferred to a second oil bath at 210 °C under carbon monoxide gas. The typical flow rate of CO gas was set at 220 mL/min and the reaction time was 30 min. The products were separated by centrifugation at 6000 rpm for 5 min and further purified by washing with ethanol three times.

Synthesis of PtCo nanoparticles with flat faces exposed (100) facets: Under argon flow, [$Pt(acac)_2$] (0.05 mmol), [$Co(acac)_2$] (0.006 mmol), oleylamine (9 mL), and oleic acid (1 mL) were mixed in a 25 mL three-necked, round-bottom flask with a magnetic stirrer. The flask was immersed in an oil bath at 130 °C, and the reaction mixture turned into a transparent solution at this temperature for 3 min. The flask was then transferred to a second oil bath at 210 °C under carbon monoxide gas. The typical flow rate of CO gas was set at 220 mL/min and the reaction time was 30 min. The products were separated by centrifugation at 6000 rpm for 5 min and further purified by washing with ethanol three times.

Catalytic test: The catalytic hydrogenation reaction was performed in a stainless steel stirred autoclave with a volume of 100 mL. The dried catalyst (2 mg), alcohol (35 mL), cinnamaldehyde (200 μL), and n-dodecane (100 μL, as an internal standard) were mixed in the autoclave. After the autoclave was sealed, H_2 was charged four times to replace air. The autoclave was heated to the reaction temperature of 23℃ and H_2 was charged to a final pressure of 2.0 MPa. The hydrogenation reaction was begun

by turning on the stirring button. The samples were periodically withdrawn from the reactor and analyzed offline with a gas chromatograph。

Characterization: X-ray diffraction (XRD) patterns of samples were recorded on a Germany Bruker D8 discover high-resolution double crystal diffractometer using Cu Kα radiation at 40 kV and 200 mA. Rietveld refinement with MDI-Jade software was used to determine the lattice constants from the XRD diffraction analysis. The morphology and size of nanomaterials were characterized using JEOL JEM-2100 Electron Microscope (JEOL, TEM, 2011, Japan) operated at 200 kV and S4800 of Hitachi. STEM images were recorded using a high-angle annular dark-field (HAADF) detector operated at JEM-ARM200F. The X-ray Photoelectron Spectroscopy (XPS) of the samples was determined on a RBD upgraded PHI-5000C. ESCA System in a high-vacuum chamber with the base pressure below 1×10^{-8} Torr. The catalytic products were analyzed by an Agilent Technologies GC-7890A instrument equipped with an Agilent Technologies 5975C insert MSD. The UV-vis spectra were recorded on a Shimadzu UV-2700 with a medium sampling scan rate and a resolution of 1 nm. The as-prepared solutions were mixed 8 μ L reaction solution with 3 mL ethanol.

Computational details Spin-polarized calculations based on density functional theory (DFT) as implemented in the Vienna ab initio Simulation Package [1-5] (VASP) exchange-correlation functional were used to evaluate the non-local exchange-correlation energy. The vacuum region between the two neighbor slabs was 13 Å, and the energy cutoff for the plane wave basis set was specified by 400 eV. The different Co-doped surfaces were modeled with the substitution of surface Pt atoms with Co. In the optimization of the surface adsorption of surfactants, all the surfaces were simulated by containing four equivalent Pt layer slabs except for Co-doped Pt (710) surface using three atom layers. The topmost two equivalent Pt layers including Co atoms are fully relaxed for all the calculations. Monkhorst-Pack[6] mesh k-points of (1× 1 × 1), (3 × 2 × 1), (2 × 1 × 1) and (3 × 1× 1) were used for Co-doped Pt(100), Co-doped Pt(110), Co-doped Pt(420) and Co-doped Pt(710) surface calculations, respectively. For the adsorption of cinnamaldehyde, all the surfaces were simulated

by containing five equivalent Pt layer slabs except for Co-doped Pt (710) surface using four atom layers, with p(3 × 3) periodicity, respectively; Co-doped Pt(710) surface was modeled with a slab in the p(3 × 1) unit cell. The topmost three equivalent Pt layers including Co atoms are fully relaxed for all the calculations. Monkhorst-Pack [2] mesh k-points of (3 × 3 × 1), (3 × 3 × 1), (2 × 2× 1) and (3 × 2× 1) were used for Co-doped Pt(100), Co-doped Pt(110), Co-doped Pt(420) and Co-doped Pt(710) surface calculations, respectively. The adsorbates and the topmost three cobalt layers are allowed to be fully relaxed. The chemisorption energy E_{ads} of the intermediate A involved in C=C and C=O hydrogenation process can be expressed as $E_{ads} = E_{A,slab} - E_{slab} - E_A$, where $E_{A,slab}$ and E_{slab} are the total energies for the slab with chemisorbed species A and the clean surface, respectively, and E_A is the energy of A in the gas phase.

Supporting Figures and Tables

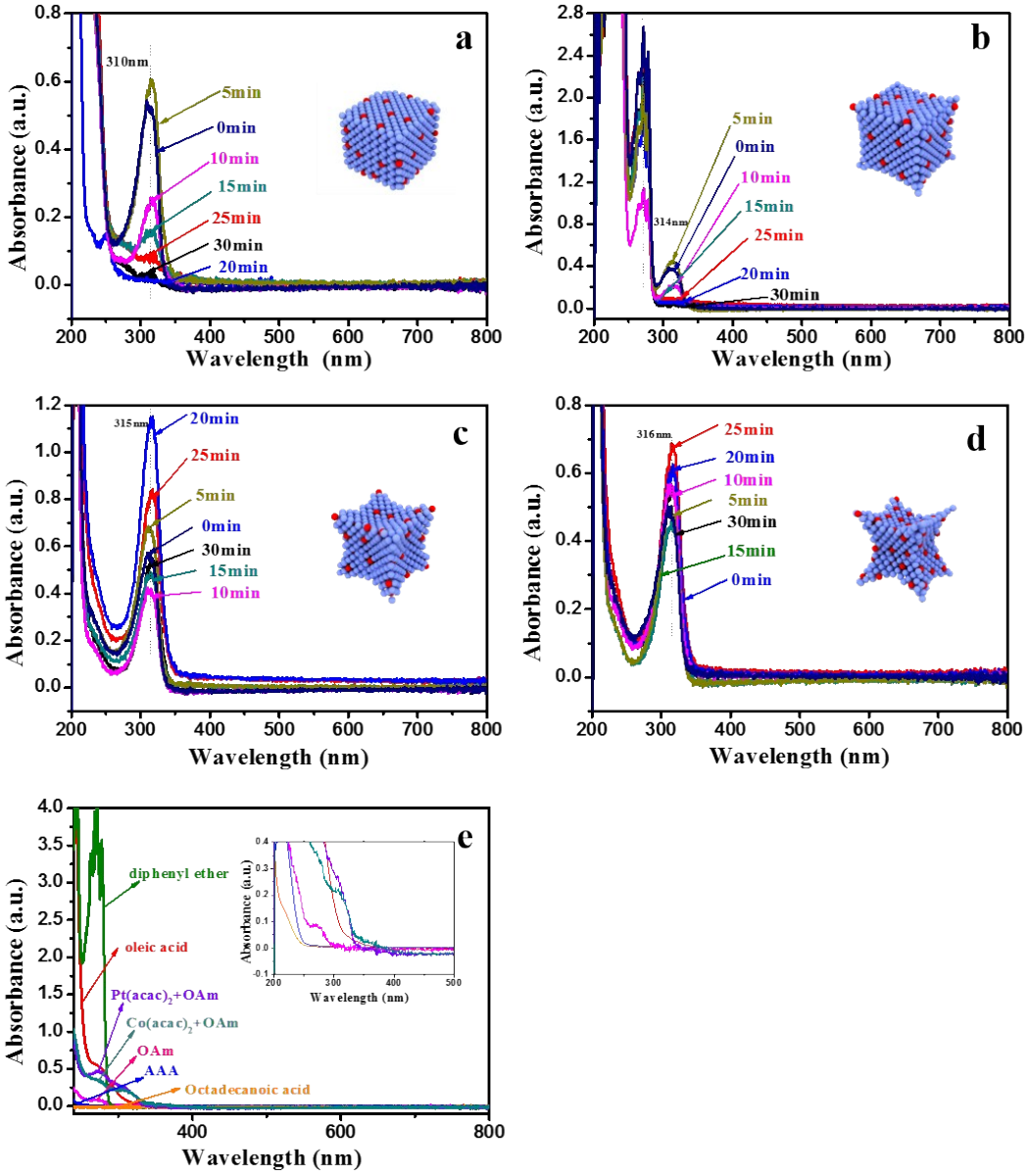

Figure S1. UV-vis spectra of the acid systems obtained after $Pt(acac)_2$ and $Co(acac)_2$ addition at different reaction times: (a) oleic acid, (b) benzoic acid and diphenyl ether, (c) adamantaneacetic acid, and (d) octadecanoic acid. (e) UV-vis spectra of the different solutions (OAm: oleylamine; AAA: adamantaneacetic acid).

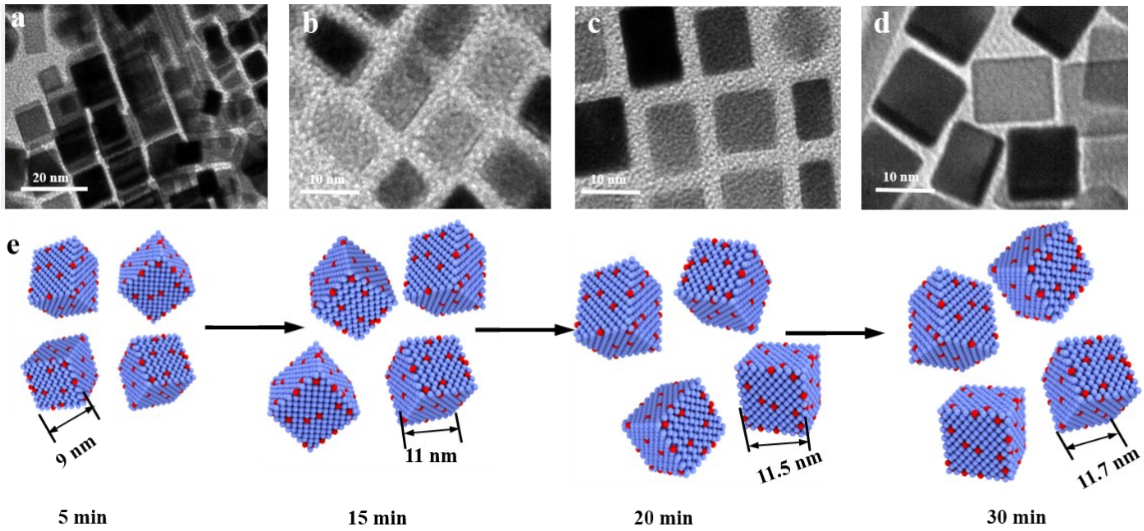

Figure S2. TEM images and in the form of $Pt_{11}Co$ nanoparticles enclosed by {100} planes under oleic acid system at different periods of times: (a) 5 min, (b) 15 min, (c) 20 min, and (d) 30 min, respectively, together with the corresponding atomic models (e).

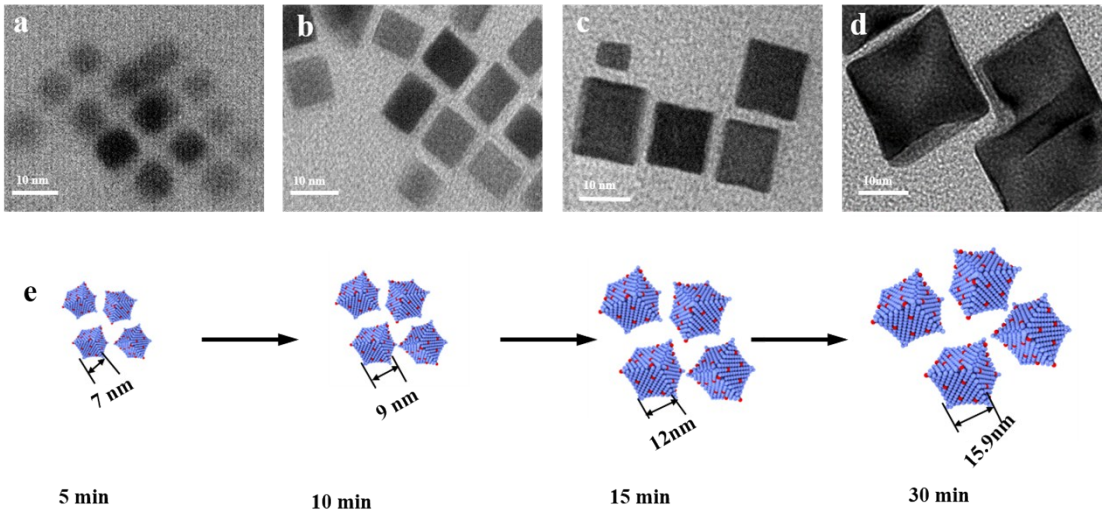

Figure S3. TEM images and in the form of $Pt_{11}Co$ nanoparticles enclosed by mainly {710} planes under benzoic acid and diphenyl ether system at different periods of times: (a) 5 min, (b) 10 min, (c) 15 min, and (d) 30 min, respectively, together with the corresponding atomic models (e).

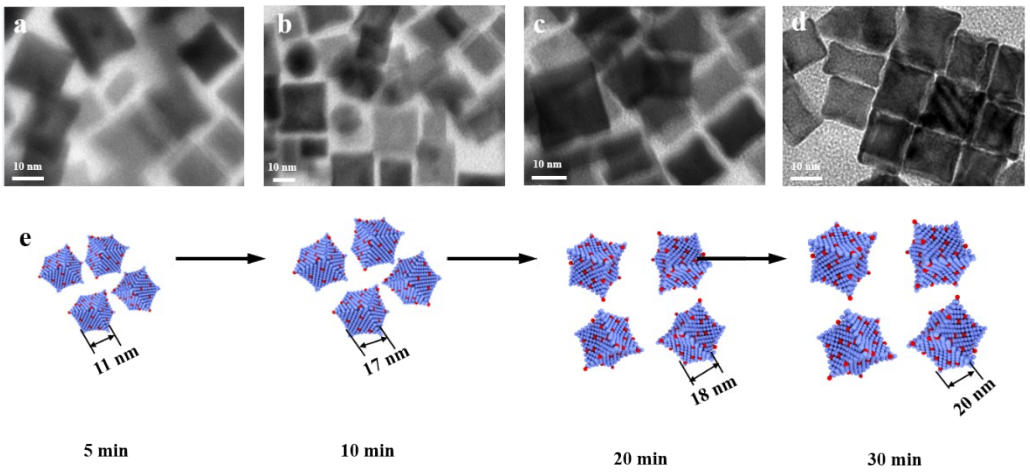

Figure S4. TEM images and in the form of $Pt_{11}Co$ nanoparticles enclosed by mainly {420} planes under adamantaneacetic acid system at different periods of times: (a) 5 min, (b) 10 min, (c) 20 min, and (d) 30 min, respectively, together with the corresponding atomic models (e).

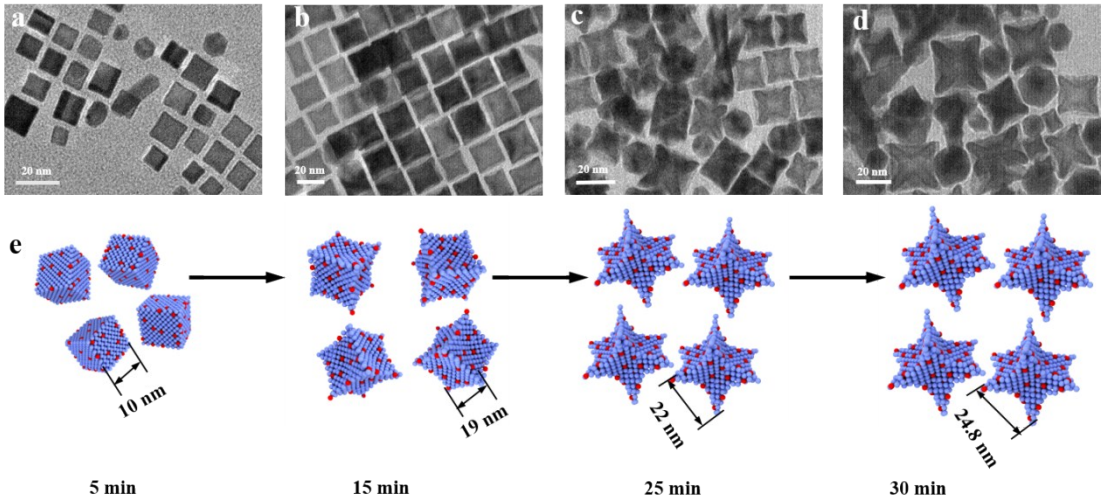

Figure S5. TEM images and in the form of $Pt_{11}Co$ nanoparticles enclosed by {110} planes under octadecanoic acid system at different periods of times: (a) 5 min, (b) 15 min, (c) 25 min, and (d) 30 min, respectively, together with the corresponding atomic models (e).

The rate of Pt or Co complex formation plays a role in the shape evolution of a Pt-Co seeds during growth. Without carboxylic acids in the solution, irregular morphologies of Pt_xCo_y nanoparticles were obtained. The carboxylic acid can bond in solution with metal ions to form a complex, which might modify the nucleation and growth steps during nanocrystal synthesis. In detail, when oleic acid is as a structure regulator, the spectrum of the complex formed in solution has a characteristic peak at 310 nm. The relative intensity of the peaks at 310 nm reached up the highest at 5 min reaction time, and then decreased with reaction time (Figure S1a). The relative intensity of the peaks reflects the content of the complex, that is, the higher is the intensity of the peaks, the higher is the content of the complex, and the less is the free metal ions. From Figure S1a, the content of the complex was quit high at the early stage, leading to the low content of free Pt or Co ions in solution, so that most of the metal atoms at the corners and edges have enough time to migrate to side faces of a cubic seed, resulting in the formation of flat surface of Pt-Co cubes. The shape evolution of Pt_xCo_y cubic seeds with time under oleic acid system also approved that the cubes were formed when the reaction time was 5 min (Figure S2). For a case of benzoic acid and diphenyl ether as a mixed-surfactant, the peak of the complex at 314 nm has the highest the relative intensity when the reaction time is about 5 min (Figure S1b). It has to point out that the peaks at 270 nm belonged to benzene compound (Figure S1e). Although the highest content of this complex formed was also appeared at the early stage, the presence of diphenyl ether slightly decreased the rate of the surface diffusion, promoting the formation of Pt-Co concave cubes enclosed by mainly {710} planes. The shape evolution of Pt_xCo_y seeds with time under benzoic acid and diphenyl ether system also suggested that the concave cubes were formed when the reaction time was 5 min (Figure S3). However, for adamantaneacetic acid as a structure agent, the peak of the complex at 315 nm reached the highest intensity at the later stage (20 min) shown in Figure S1c, implying that the amount of free metal ions in solution was large, therefore most of metal atoms were confined to the corner sites and a small portion of metal atoms at the corners migrated to the edges, leading to the formation of curved faces of Pt-Co nanoparticles with mainly exposed (420)

facets. Figure S4 indicated that under benzoic acid and diphenyl ether system, the concave cubes were also formed when the reaction time was 20 min. In the solution of octadecanoic acid as a surfactant, the peak of the complex at 316 nm formed in solution achieved the highest relative intensity at 25 min (Figure S1d). Thus a little more portion of metal atoms at the corners migrated to the edges, resulting in the production of Pt-Co nanoparticles enclosed by {110} facets. The formation of PtCo_(110) nanoparticles also was found to be formed at 25 min, shown in Figure S5.

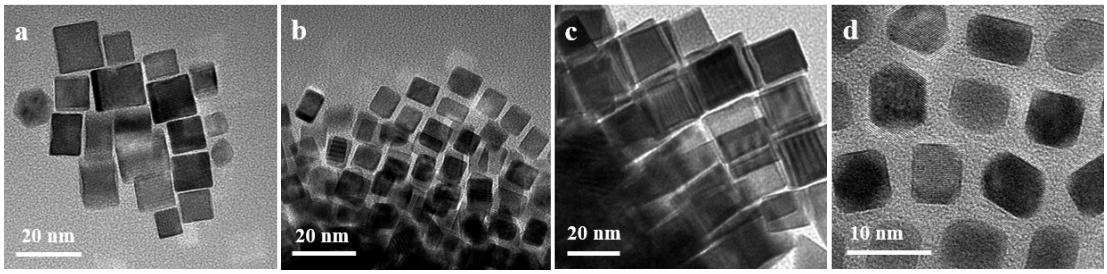

Figure S6. TEM images of pure Pt nanoparticles as-synthesized using carboxylic acids as surfactants: (a) octadecanoic acid, (b) benzoic acid or adamantaneacetic acid, (c) benzoic acid and diphenyl ether, and (d) oleic acid, respectively.

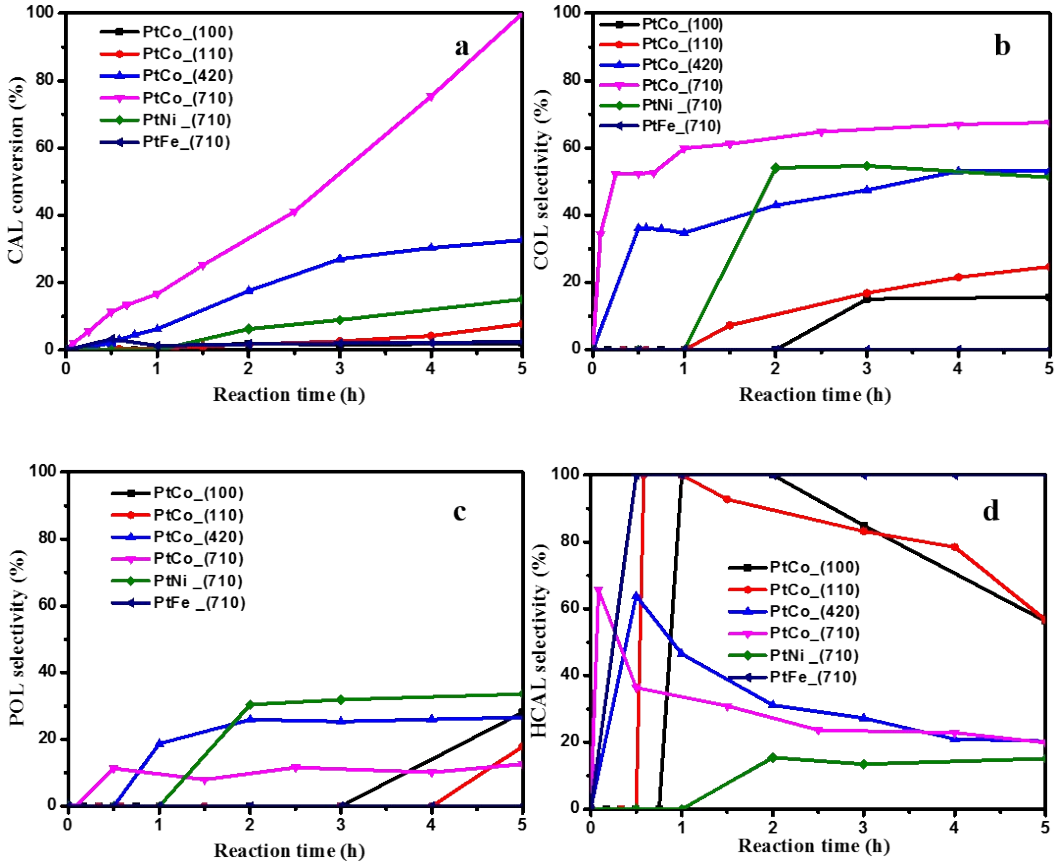

Figure S7. Catalytic results of $Pt_{11}Co$, $Pt_{11}Ni$ and $Pt_{11}Fe$ nanoparticles for the selective hydrogenation of cinnamnldehyde as a function of reaction time. (CAL:cinnamaldehyde; COL:cinnamicalcohol; HCAL:phenylpropyl aldehyde; POL:phenylpropanol)

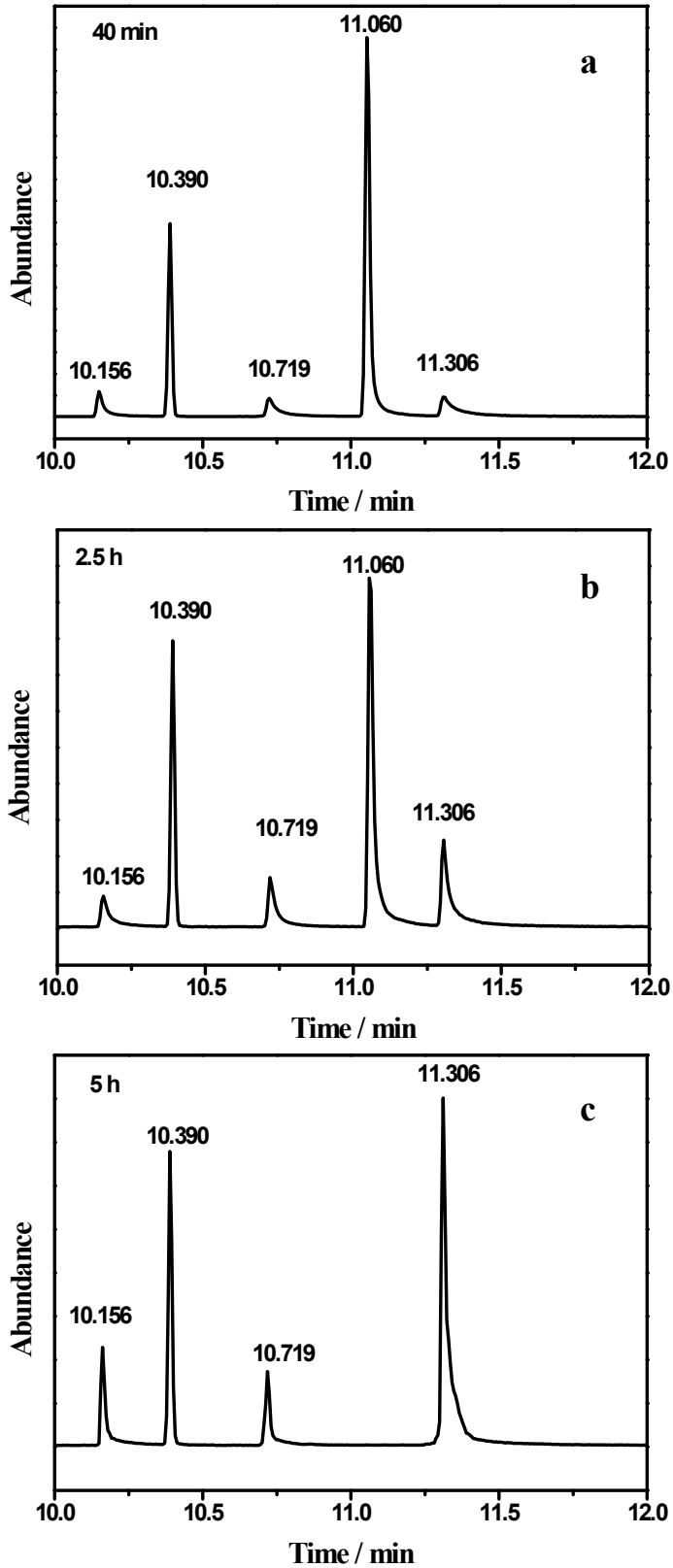
40 min
11.060
a
10.390
Abundance
10.156
10.719
11.306
10.0
10.5
11.0
11.5
12.0
Time / min
2.5 h
11.060
b
10.390
Abundance
10.719
11.306
10.156
10.0
10.5
11.0
11.5
12.0
Time / min
5 h
11.306
c
10.390
Abundance
10.156
10.719
10.0
10.5
11.0
11.5
12.0
Time / min

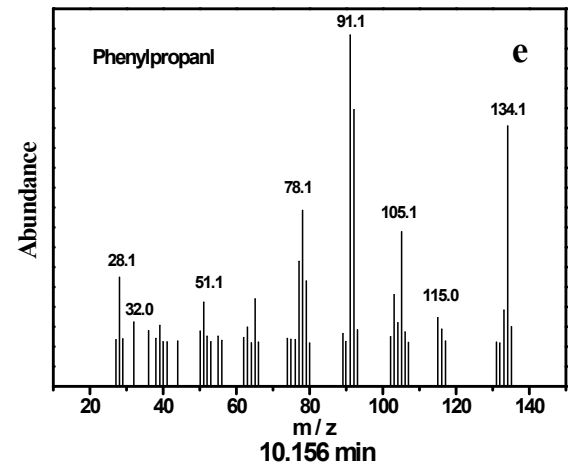
Phenylpropanl
e
91.1
134.1
78.1
105.1
28.1
51.1
115.0
32.0
Abundance
20
40
60
80
100
120
140
m / z
10.156 min

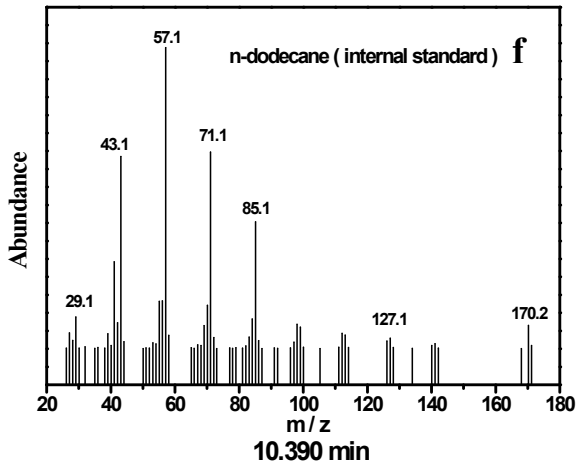
n-dodecane (internal standard)
f
57.1
43.1
71.1
85.1
29.1
127.1
170.2
Abundance
20
40
60
80
100
120
140
160
180
m / z
10.390 min

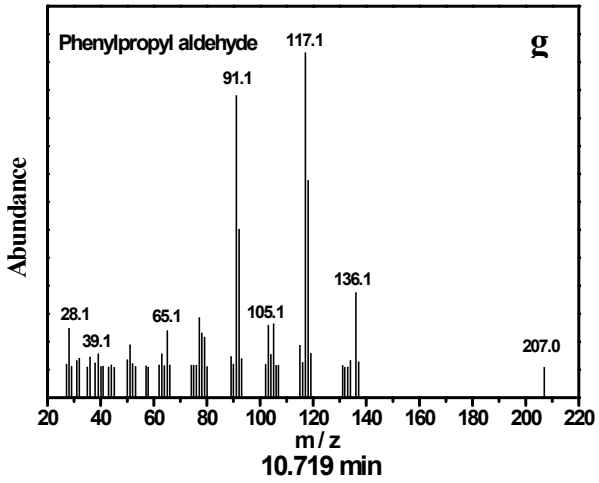
Phenylpropyl aldehyde
g
117.1
91.1
136.1
28.1
65.1
105.1
39.1
207.0
Abundance
20
40
60
80
100
120
140
160
180
200
220
m / z
10.719 min

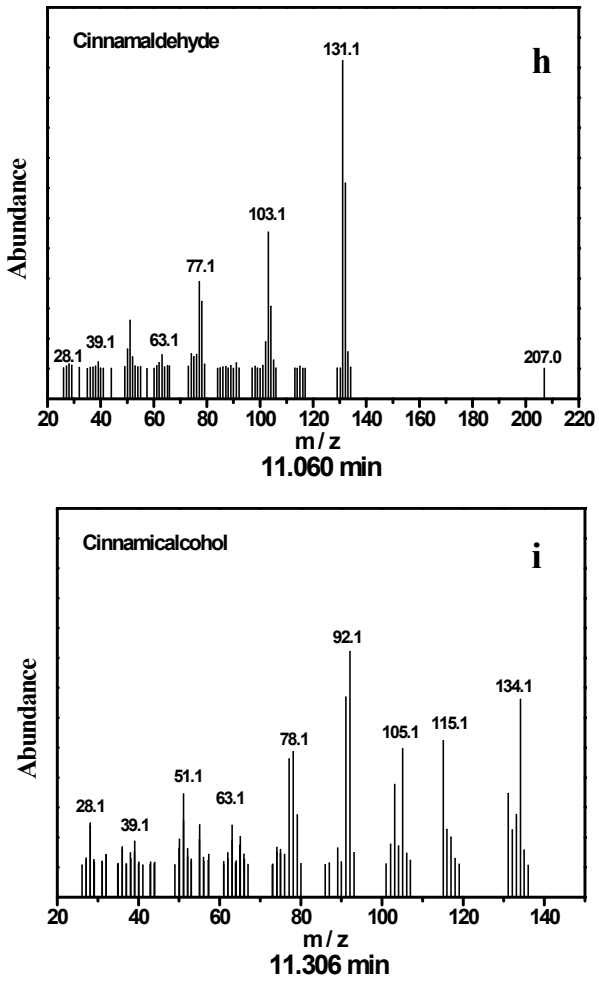

Figure S8. (a-c) GC trace of the crude product arising from hydrogenation of cinnamnldehyde with time over PtCo_(710) nanoparticles. (e-i) Mass spectra of the crude product arising from hydrogenation of cinnamnldehyde over PtCo_(710) nanoparticles.

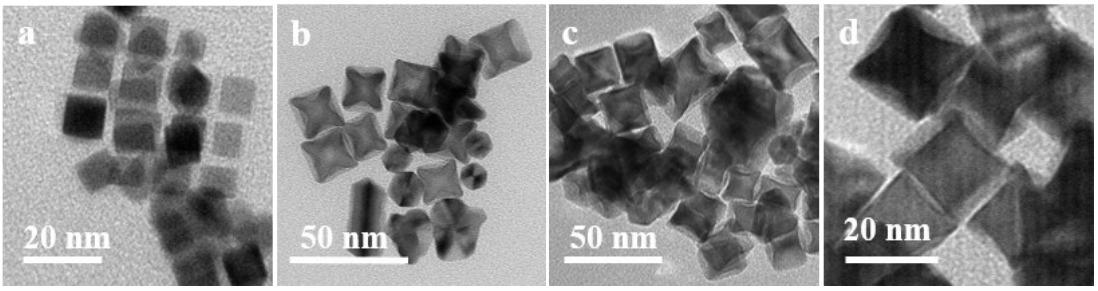

Figure S9. TEM images of $Pt_{11}Co$ nanoparticles after catalytic reactions: (a) $Pt_{11}Co$_(100), (b) $Pt_{11}Co$_(110), (c) $Pt_{11}Co$_(420) and (d) $Pt_{11}Co$_(710).

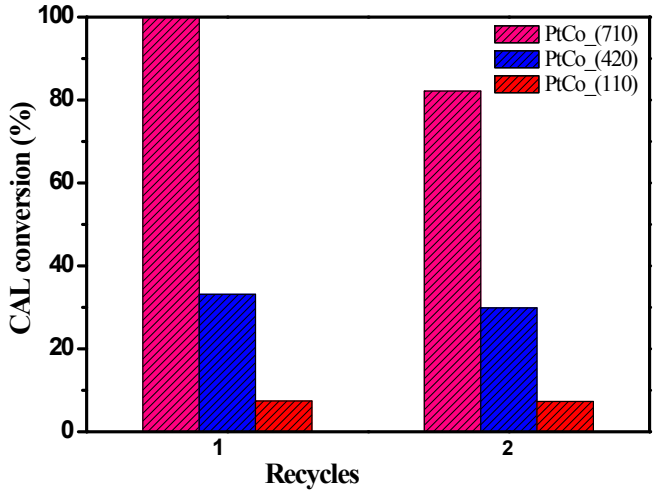

Figure S10. Catalytic activity of spent Pt-based bimetal nanoparticles for the catalytic hydrogenation of cinnamnldehyde.

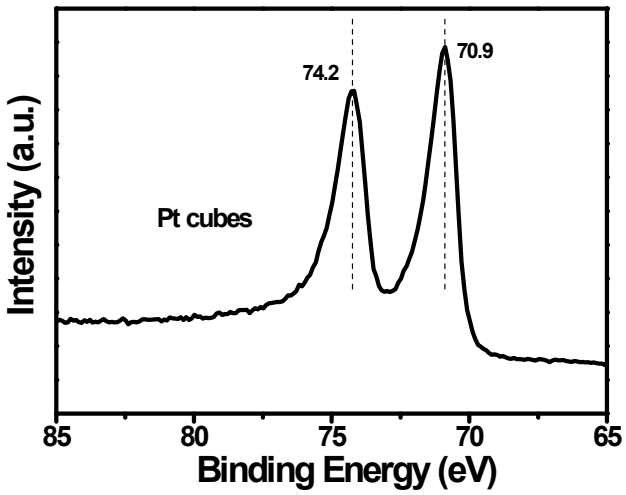

Figure S11. Pt 4f electron region of XPS profile of Pt nanocubes.

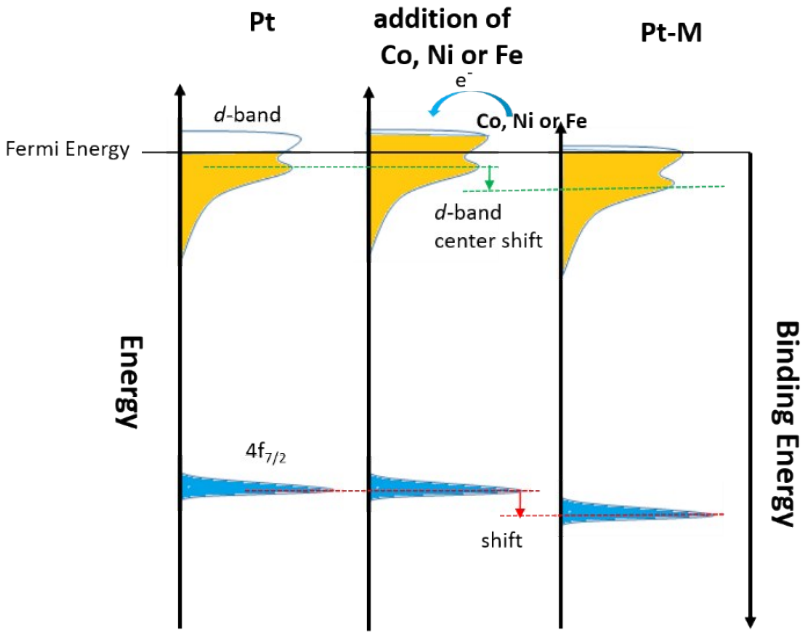

Figure S12. Schematic explanation of the addition of Co, Ni, Fe on the electronic structures of Pt.[7]

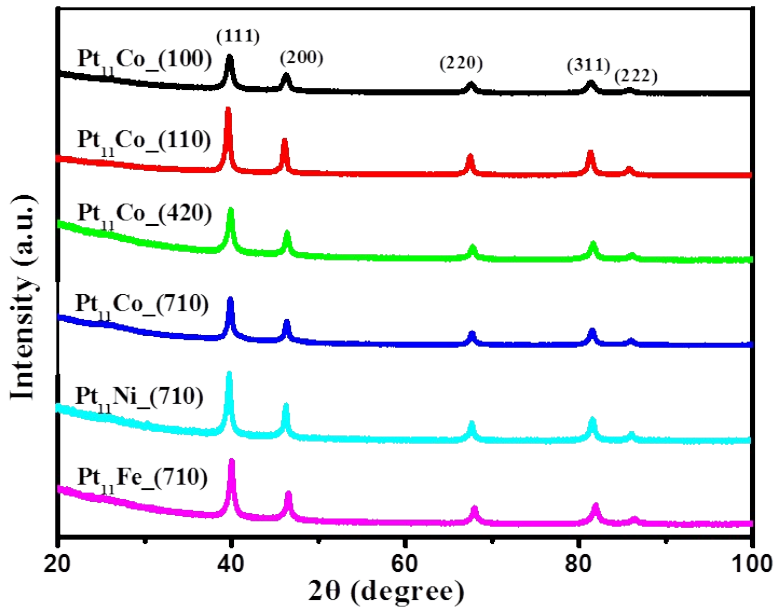

Figure S13. XRD patterns of the $Pt_{11}Co$, $Pt_{11}Ni$, $Pt_{11}Fe$ nanoparticles enclosed by different facets.

Table S1. Diffractive data of samples.

Samples	2θ (°)					Cell constant ***a*** (Å)
	(111)	(200)	(220)	(311)	(222)	
pure Pt	39.754	46.233	67.452	81.242	85.688	3.92
pure Co	44.216	51.522	75.853	92.224	97.657	3.55
$Pt_{11}Co$_(100)	39.788	46.268	67.516	81.383	85.872	3.91
$Pt_{11}Co$_(110)	39.788	46.268	67.614	81.484	85.973	3.91
$Pt_{11}Co$_(420)	39.888	46.369	67.715	81.586	86.175	3.90
$Pt_{11}Co$_(710)	39.918	46.470	67.759	81.802	86.190	3.90
$Pt_{11}Ni$_(710)	39.898	46.203	67.743	81.666	85.905	3.90
$Pt_{11}Fe$_(710)	39.898	46.547	67.916	82.010	86.322	3.90

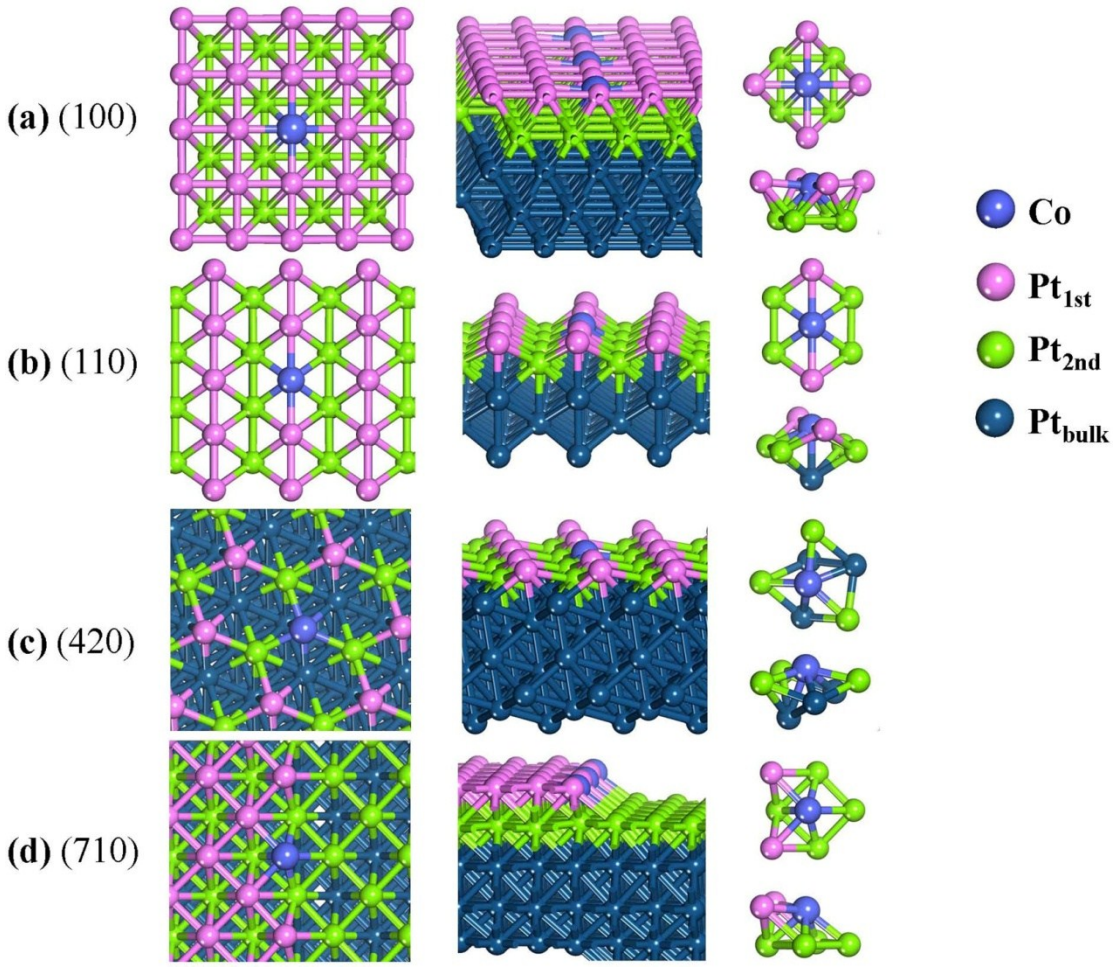

Figure S14. The representative surface atomic configurations for Co-doped (100), (110), (420) and (710) surfaces. (Pt atoms in the first layer (Pt_{1st}) and in the second layer (Pt_{2nd}) and in the bulk are in magenta, green and darkcyan. Co atoms are in blue.)

Table S2. Calculated bond lengths (Å) of cinnamaldehyde adsorption on the Co-doped Pt (100), (110), (420) and (710) surfaces.

Surface	d_{O-Co}	d_{C1-Pt}	d_{C2-Pt}	d_{C3-Pt}	$d_{O=C1}$	d_{C1-C2}	$d_{C2=C3}$
Co-doped Pt (100)	1.92	2.30	2.16	2.16	1.32	1.44	1.46
Co-doped Pt (110)	1.90	2.17	2.24	2.24	1.34	1.46	1.47
Co-doped Pt (420)	1.86	2.18	2.24	2.16	1.35	1.48	1.43
Co-doped Pt (710)	1.93	-	2.20	2.16	1.28	1.45	1.44

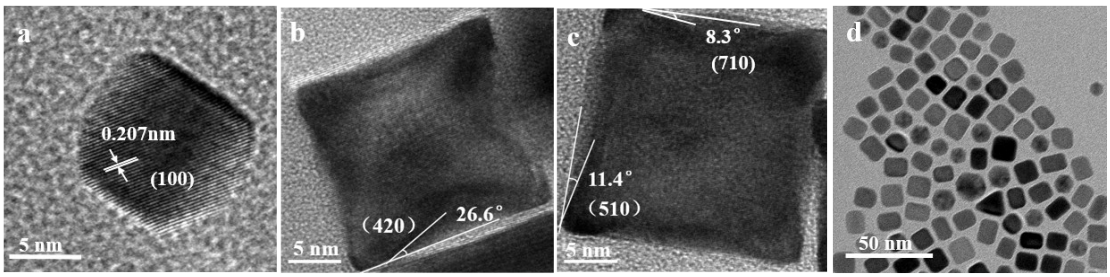

Figure S15. TEM images of Pt_xNi_y nanoparticles using carboxylic acids as: (a) octadecanoic acid, (b) benzoic acid or adamantaneacetic acid, (c) benzoic acid and diphenyl ether, and (d) oleic acid, respectively.

From Figure S15a, Pt_xNi_y nanocubes without concave structure were synthesized under octadecanoic acid system. As well Pt_xNi_y nanocubes also were made under oleic acid system, shown in Figure S15d. While Pt_xNi_y concave nanocubes enclosed by mainly (420) planes can be prepared under the benzoic acid or adamantaneacetic acid system (Figure S15b). Pt_xNi_y concave nnaocubes enclosed by mainly (710) planes can be made under the system of benzoic acid and diphenyl ether (Figure S15c).

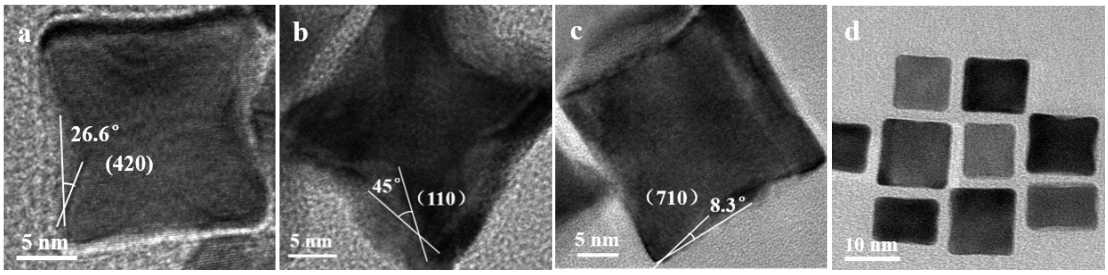

Figure S16. TEM images of Pt_xFe_y nanoparticles using carboxylic acids as surfactants: (a) octadecanoic acid, (b) benzoic acid or adamantaneacetic acid, (c) benzoic acid and diphenyl ether, and (d) oleic acid, respectively.

From Figure S16a, under the system of octadecanoic acid, Pt_xFe_y concave nanocubes enclosed by mainly (420) planes can be prepared; from Figure S16b, under benzoic acid or adamantaneacetic acid, Pt_xFe_y concave nanocubes bounded by (110) planes can be synthesized; from Figure S16c, under the system of benzoic acid and diphenyl ether, Pt_xFe_y concave nanocubes enclosed by mainly (710) planes were synthesized. Under the system of oleic acid, Pt_xFe_y nanocubes were synthesized (Figure S16d).

References

1. P. E. Blöchl, *Phys. Rev. B* 1994, **50**, 17953-17979.
2. G. Kresse and J. Hafner, *Phys. Rev. B* 1993, **47**, 558-561.
3. G. Kresse and J. Furthmuller, *Phys. Rev. B* 1996, **54**, 11169-11186.
4. G. Kresse and D. Joubert, *Phys. Rev. B* 1999, **59**, 1758-1775.
5. J. P. Perdew, K. Burke and M. Ernzerhof, *Phys. Rev. Lett.* 1996, **77**, 3865-3868.
6. H. J. Monkhorst and J. D. Pack, *Phys. Rev. B* 1976, **13**, 5188–5192.
7. M. Wakisaka, S. Mitsui, Y. Hirose, K. Kawashima, H. Uchida and M. Watanabe, *J. Phys. Chem. B* 2006, **110**, 23489-23496.